Superhydrophobic PVDF/SiO_2 composite films with a hierarchical structure for highly stabilized radiative cooling

Zhengfei Tan,[a,c] Huiyu Yang,[a*] Xiaohua Cheng,[a] Guowen Yu,[a] Hai Liu,[a] Bingqing Zhang,[b*] Chunli Gong,[a]

[a] School of Chemistry and Materials Science, Hubei Engineering University, Xiaogan 43200, China.

[b] State Key Laboratory of Marine Resource Utilization in South China Sea, School of Materials Science and Engineering, Hainan University, HaiKou 570228, China.

[c] Ministry of Education Key Laboratory for the Green Preparation and Application of Functional Materials, Hubei Key Laboratory of Polymer Materials, School of Materials Science and Engineering, Hubei University, Wuhan 430062, China.

* Corresponding author: hy-yang_wtu@hotmail.com (H. Yang) and bqzhang@hainanu.edu.cn (B. Zhang)

Experimental section

Materials

Polyvinylidene fluoride (PVDF, Mw~180000) was obtained from Sigma-Aldrich. Hydrophobic fumed nano silica (SiO_2, 98%, particle size 7-40 nm, specific surface area: 260 m^2/g) and N, N-dimethylacetamide (DMAC) were purchased from Aladdin Reagent Co., Ltd. Acetone (CH_3COCH_3, AR) was supplied from Tianjin Fuyu Fine Chemical Co., Ltd. Deionized water for experiments was supplied through a seepage source water purifier (SYEL-I-200L, Chengdu Seepage Source Technology Co., Ltd.) with a resistivity of 10-16 MΩ·cm at room temperature. Commercial cooling materials were purchased from local stores.

Preparation of PVDF/SiO_2 thin films

PVDF was dissolved in a mixed solvent comprising N, N-dimethylacetamide and acetone. Then, an appropriate amount of SiO_2 nanoparticles was added to the PVDF solution and stirred in a water bath at 45 °C for 15 min. The mass ratios of SiO_2 to PVDF were 5 wt.%, 10 wt.%, 15 wt.% and 20 wt.%, respectively. After mixing, deionized water was added and stirred to form a homogeneous precursor solution. The mass ratio of PVDF: acetone: DMAC: water was 4:40:4:5. Finally, the precursor solution was poured into a flat glass mold and scraped into a thin coating with a fixed height spatula. Subsequently, the mold was immersed in an ice water bath for 10 min and then dried in a vacuum drying oven at 60°C for 24 h to obtain the PVDF-n%SiO_2 composite film. The n represents the mass ratio of SiO_2 to PVDF.

Characterization

The surface microscopic morphology of PVDF-n%SiO_2 composite film was observed using scanning electron microscopy (SEM, JSM-6510LV, JEOL Co. Ltd., Japan). The surface topography of the composite film was revealed by AFM (Bruker, Billerica, MA, USA) in tapping mode with a scanning range of 5 μm × 5 μm.

The static water contact angle of the PVDF-n%SiO_2 composite membrane surface was tested using a Dataphysics OCA 30 (Dataphysics, Germany) contact angle system. The surface energies of the PVDF and PVDF-n% SiO_2 were measured using droplets of distilled water and diiodomethane. The values can be derived directly with the Krüss DSA100s or according to the Wu model[1,2].

$$[\frac{\gamma_S^d\gamma_L^d}{(\gamma_S^d+\gamma_L^d)}+\frac{\gamma_S^p\gamma_L^p}{(\gamma_S^p+\gamma_L^p)}]=0.25\gamma_L(1+cos\theta) \quad (1)$$

$$\gamma_L=\gamma_L^d+\gamma_L^p \quad (2)$$

$$\gamma_S=\gamma_S^d+\gamma_S^p \quad (3)$$

where γ_L^d、γ_L^pdenote the polar component and dispersion component of liquid surface tension, respectively; θ is the contact angle； γ_S^p is the solid dispersion component; γ_S^d is the solid polar component.

The reflectance spectra of the composite films in the UV-Vis-NIR (200-2500 nm) range were analyzed using a Shimadzu UV-3600 spectrometer with an integrating sphere. The FTIR spectrometer with gold integrating sphere (Nicolet iS50, Thermo Fisher Scientific, USA) was used to test the reflectance of the composite films in the range of 2.5 to 25 μm. Reflectance was measured over a polarization angle range of 10° to 80° using a polarizer on an infrared spectrometer equipped with an intelligent diffuse reflectance attachment.

The tensile strength of PVDF-n%SiO_2 composite films was analyzed by a universal testing machine (Instron 5965, Norwood, MA, USA). The tensile speed and clamping distance were 5 mm/min and 2 cm, respectively. Each group of samples was subjected to at least three parallel experiments.

The thermal conductivity of the PVDF-n% SiO_2 composite films was measured by a thermal constant analyzer (TPS 2500S, Hot Disk, Sweden) at room temperature.

The daytime radiative cooling performance of the PVDF-n% SiO_2 composite films was evaluated by a homemade device. Samples with a diameter of 6 cm were placed on the surface of polystyrene foam, while the other parts were wrapped by aluminum foil to reduce the solar heat gain of the device. To minimize heat convection and heat conduction, the top was covered with a transparent polyethylene (PE) film to form a sealed space. Under the polyethylene (PE) film, a digital thermometer (PM6501, China Huayi Instrument Co., Ltd.) with K-type thermocouples was used to record the temperature of the chamber under the sample cover. The real time intensity was recorded by a solar densitometer (TES 132). Daytime radiative cooling power calculations for the composite membrane are shown in Note S1. Meanwhile, a xenon lamp (CEL-HXF300, Zhong Jinyuan Technology Co., Ltd. China) with 1000 $W \cdot m^{-2}$ radiant intensity was used to simulate sunlight to further evaluate the radiative cooling performance of the samples. The infrared images were obtained from a portable infrared thermal imager (TiS65, Fluke, USA).

The abrasion fastness of the composite films was evaluated by the available reports.[3] Composite films with 50 g weights fixed to the surface were placed on 400

mesh sandpaper and then moved back and forth across the sandpaper more than 50 times at a speed of 1 cm/s. The UV aging of the composite films was performed by continuous irradiation under UV light with a radiation intensity of 400 $W \cdot m^{-2}$ for 20 h and 168 h. The distance between the sample and the center of the light source (UV lamp, 125 W, 365 nm) was 20 cm. After the abrasion fastness test and UV aging, the static water contact angle and radiative cooling properties of the films surface were measured.

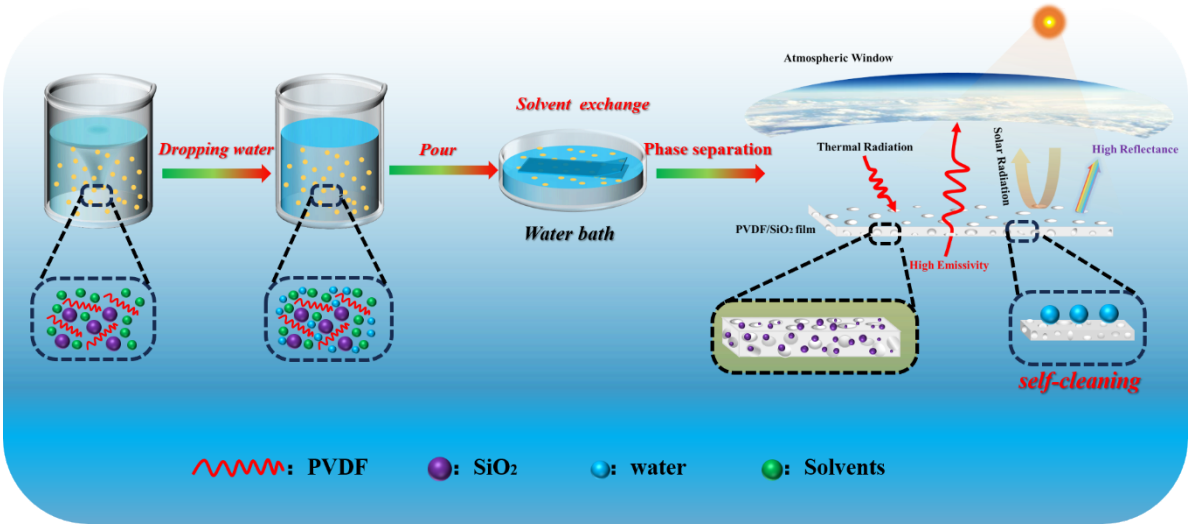

Fig. S1 Schematic of the preparation of PVDF/SiO_2 composite films with hierarchical structure for radiation cooling.

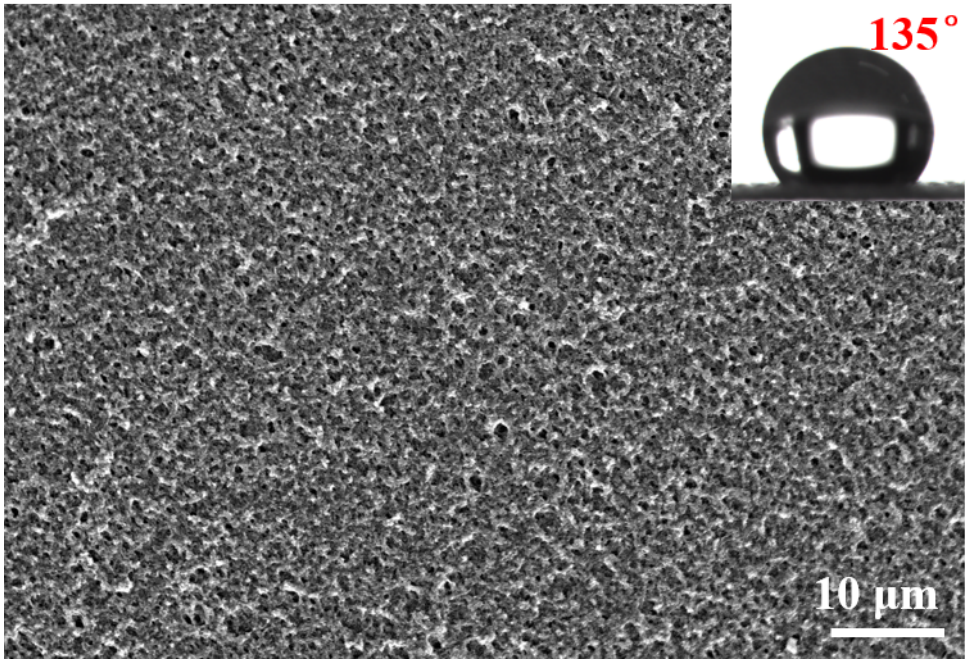

Fig. S2 Surface micromorphology and static water contact angle of PVDF films.

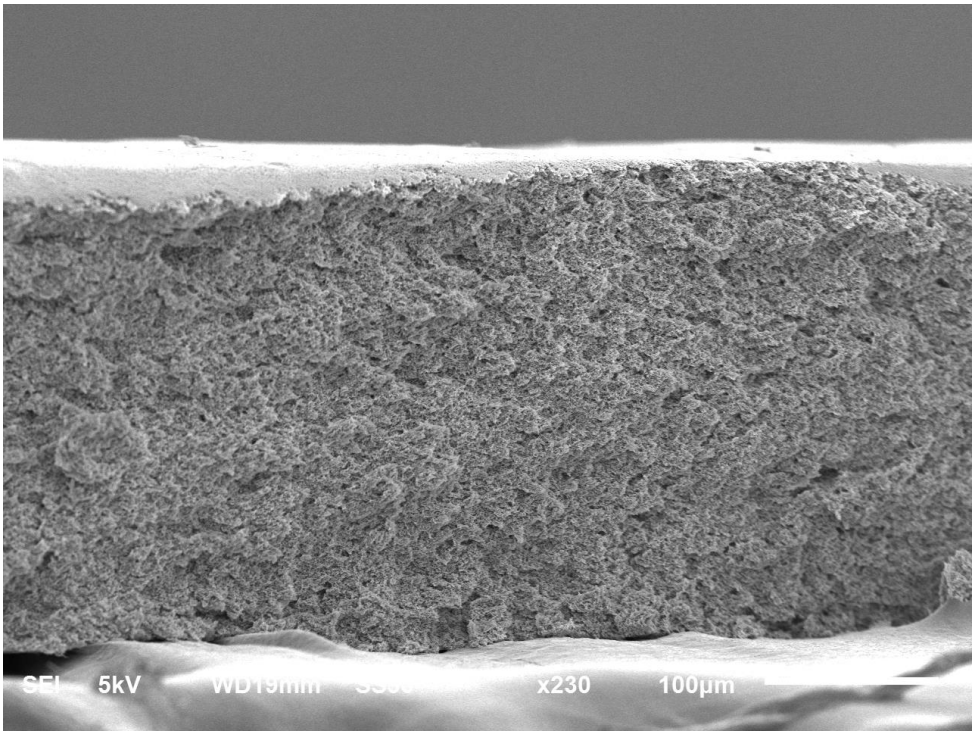

Fig. S3 Cross-sectional SEM image of PVDF-10% SiO_2 composite film.

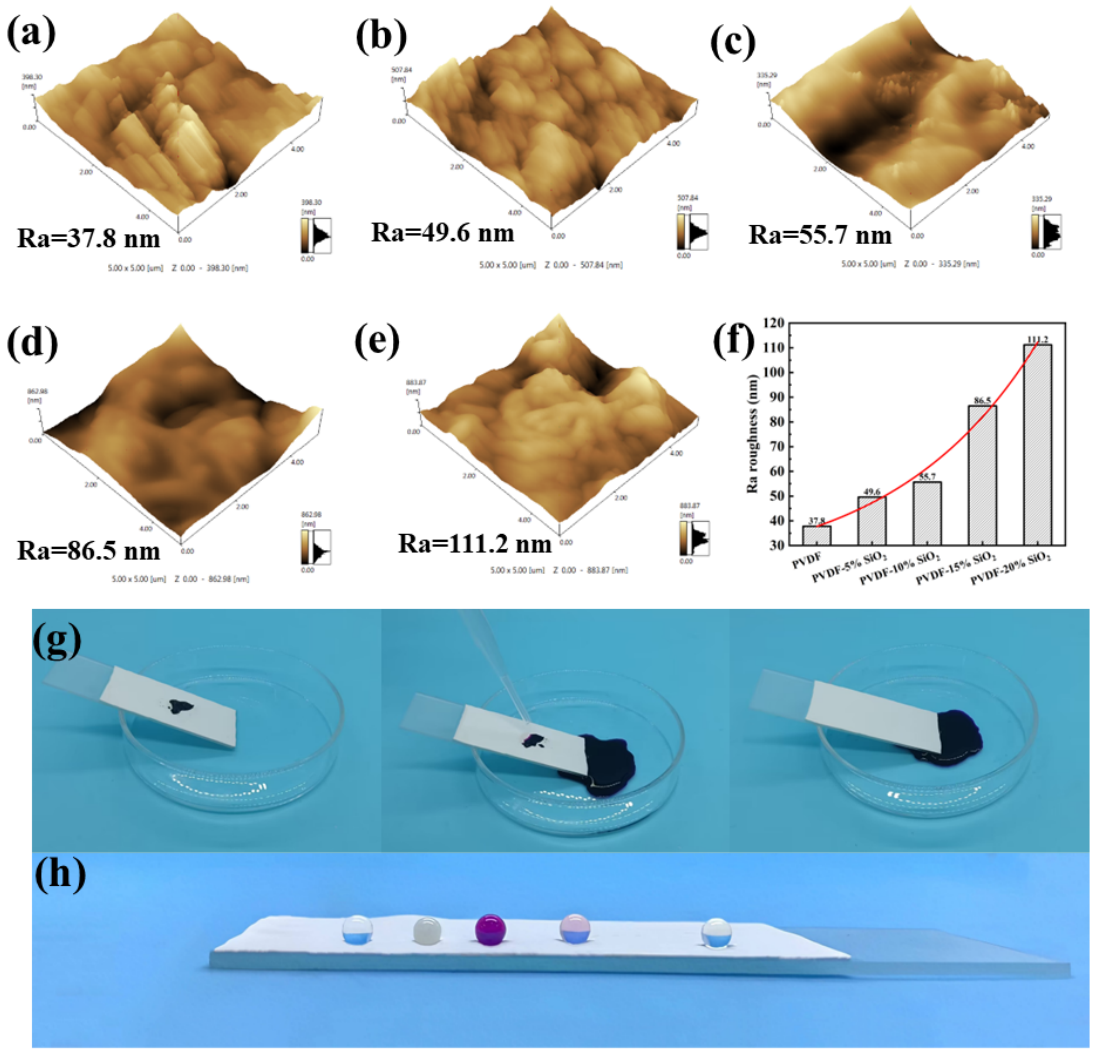

Fig. S4 AFM image of PVDF and PVDF-n% SiO_2 composite films: a) PVDF; b) PVDF-5% SiO_2; c) PVDF-10% SiO_2; d) PVDF-15% SiO_2; e) PVDF-20% SiO_2; f) Surface roughness (Ra); g) Optical photograph of dye liquid droplets slipping on PVDF-10%SiO_2 composite film; h) Optical photographs of drops of deionized water, milk, potassium permanganate solution, phenolphthalein and tea on the surface of PVDF-10%SiO_2 composite membrane;

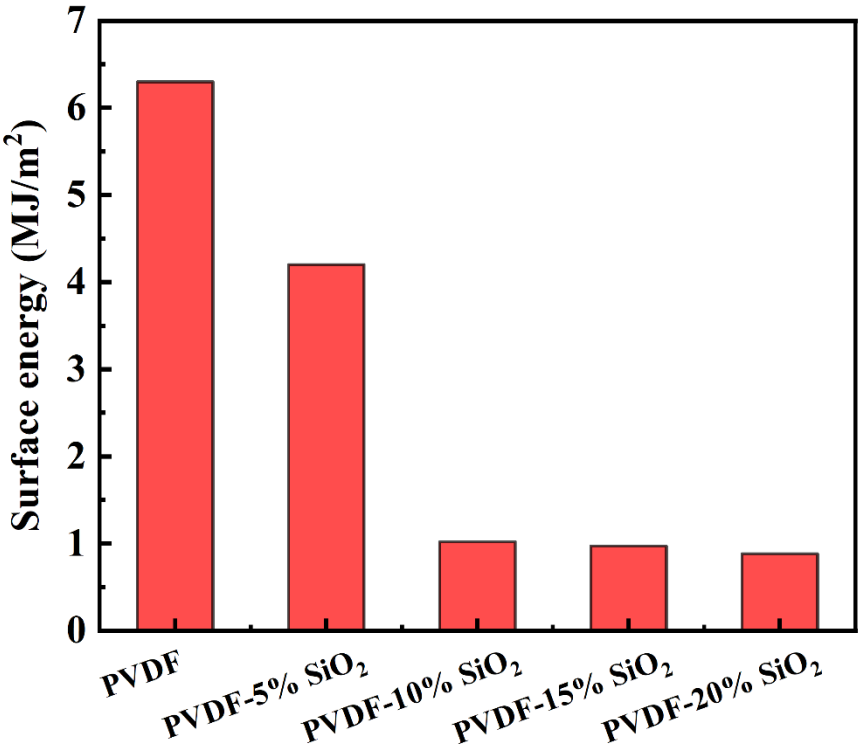

Fig. S5 Surface energy of PVDF and PVDF-n% SiO_2 composite films.

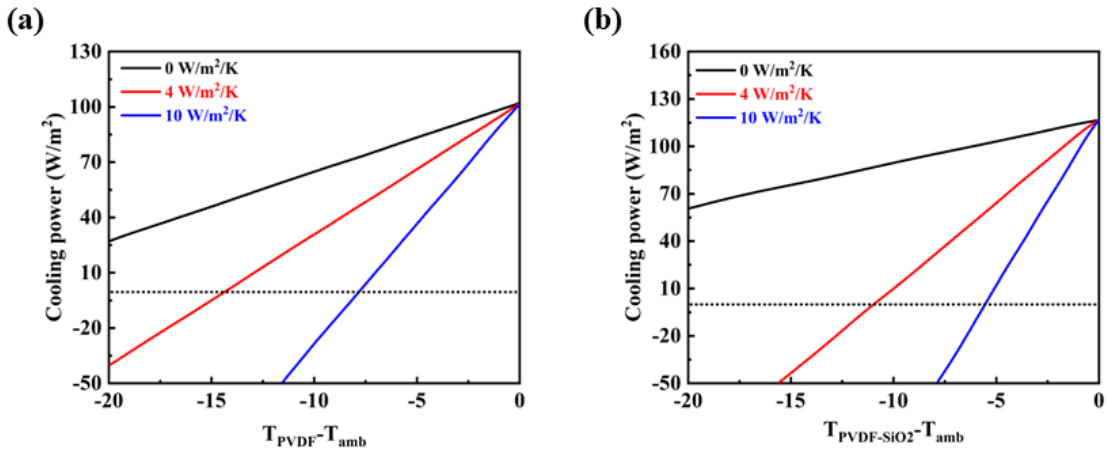

Fig. S6 a) and b) are the radiative cooling powers of PVDF and PVDF/SiO_2 composite membranes, respectively. The effective conduction-convection heat constants (hc) are 0, 4 and 10 W/m^2/K (Ambient temperature for 35°C).

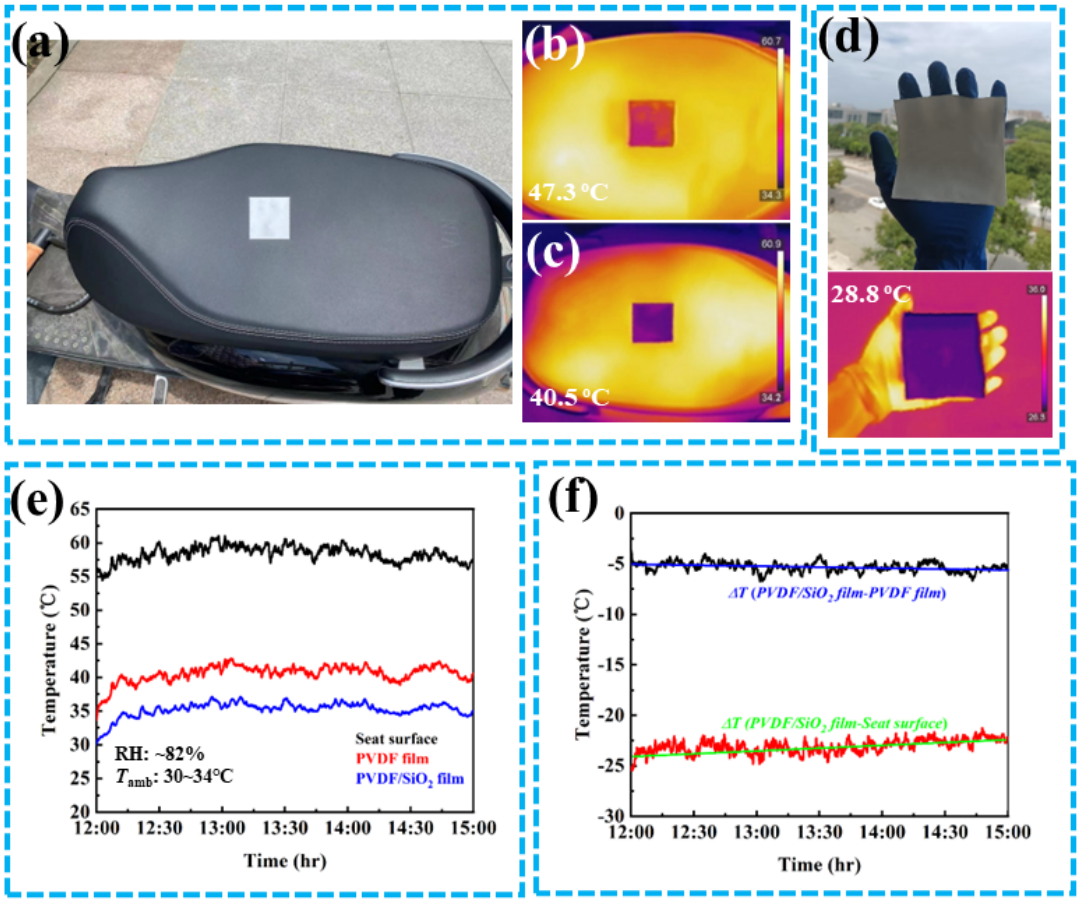

Fig. S7 a) Photographs of PVDF/SiO_2 composite films covered with electric-bike seats; b) and c) are infrared images of PVDF film and PVDF/SiO_2 composite film covered on a black seat, respectively; d) Photographs of PVDF/SiO_2 composite films placed on hands and infrared images after 5 min of direct sunlight; e) and f) are the real-time temperatures and the corresponding temperature differences of the seat surfaces with and without film coverage under direct sunlight, respectively (July 23, 2023, Xiaogan, China, 30°55′N, 113°54′E, RH:~82%, T_{amb}: 30-34°C)

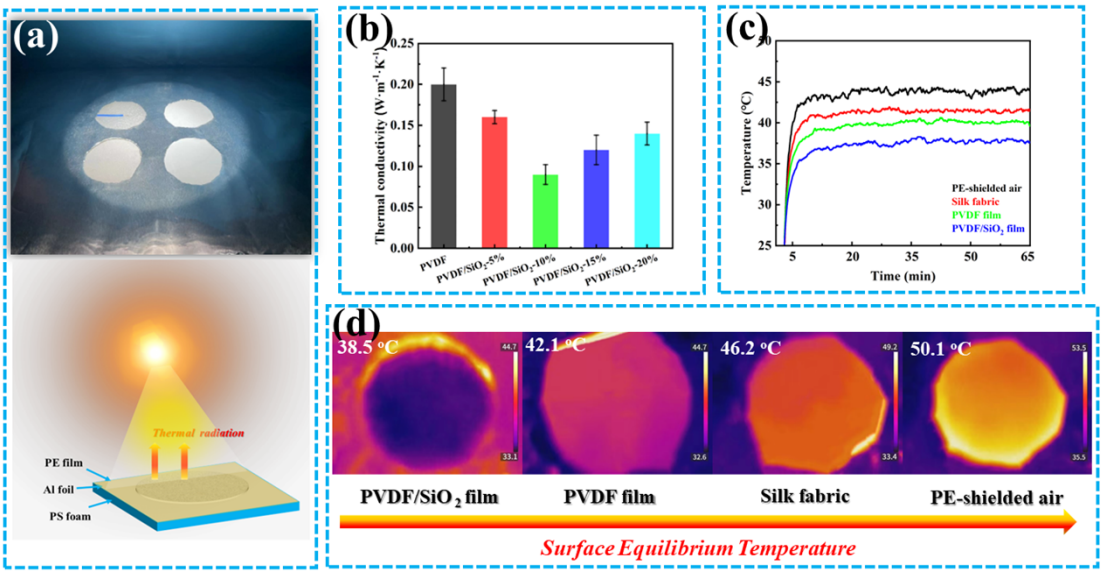

Fig. S8 a) Photograph of the setup for testing radiative cooling by xenon lamp simulating sunlight; b) Thermal conductivity of PVDF and PVDF-n%SiO_2 composite films; c-d) Real-time temperature profile of the film-covered cavity and Infrared thermograms of the equilibrium temperature of the film surface under xenon lamp simulated sunlight irradiation, respectively.

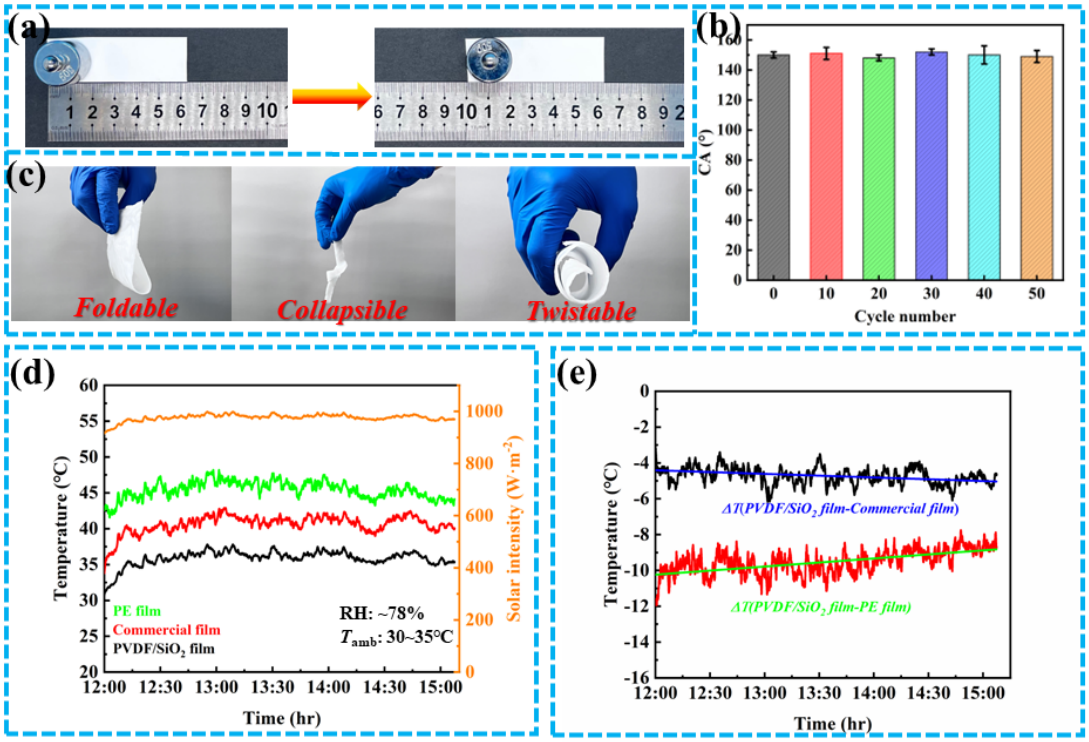

Fig. S9 a) Photographs of mechanical stability tests of PVDF/SiO_2 composite film; b) Contact angle of PVDF/SiO_2 composite film after multiple cycles of abrasion resistance; c) Flexibility test of PVDF/SiO_2 composite film; d) Real-time temperature and insolation intensity of outdoor radiative cooling of PVDF/SiO_2 composite film (after 50 cycles of abrasion) and commercial film (August 10, 2023, Xiaogan, China, 30°55′N, 113°54′E, RH:~78%, T_{amb}: 30-35°C). e) Temperature drop (ΔT) of PVDF/SiO_2 composite film with commercial film and PE covered cavity, respectively.

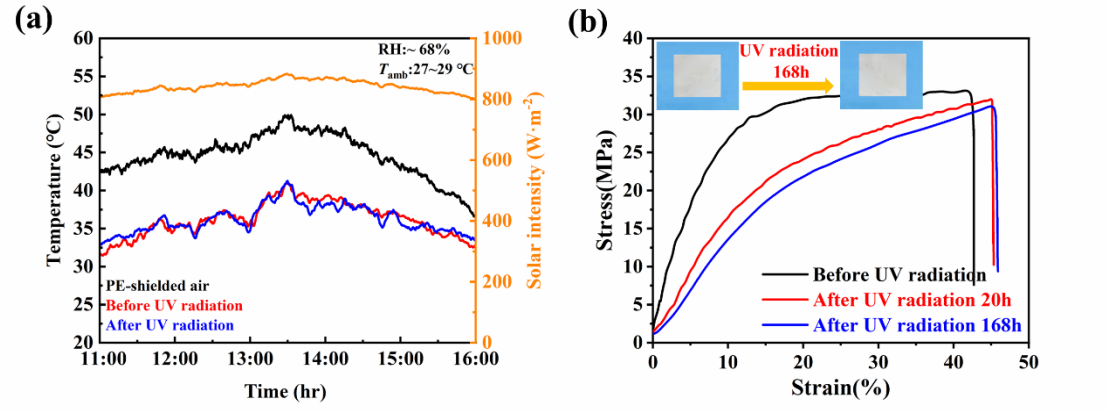

Fig. S10 a) Real-time temperature and insolation intensity of outdoor radiative cooling of PVDF/SiO_2 composite film before and after UV radiation (UV radiation 168 h, 400 W·m^{-2}) (October 10, 2023, Xiaogan, China, 30°55′N, 113°54′E，RH:~68%, T_{amb}: 27-29°C); b) Stress-strain curves of PVDF/SiO_2 composite film before and after UV radiation (UV radiation 168 h and 20h) (Inset PVDF/SiO_2 composite film before and after UV radiation for 168h).

Note S1:

When PVDF and PVDF/SiO_2 composite films are exposed to the clear sky, its surfaces absorb solar and atmospheric thermal radiation while radiating heat into outer space.[4] Meanwhile, due to the temperature difference, heat is transferred from the environment to the PVDF and PVDF/SiO_2 composite films in the form of thermal conduction and convection.[5,6] Based on the conservation of energy, the net cooling power of the film is expressed as:

$$P_{cool}(T) = \mathrm{P}_{\mathrm{r}\,ad}(T) - P_{sun} - P_{atm}(T_{amb}) - P_{cond+conv} \quad \backslash*$$

MERGEFORMAT (1)

Where T and A are the absolute temperature and surface area of the PVDF and PVDF/SiO_2 composite films surface, respectively. T_{amb} is the ambient temperature. $P_{rad}(T)$ is the power of thermal radiation of the films, $\mathrm{P}_{\mathrm{sun}}$ is the heat power density produced by absorbing solar energy, P_{atm} (T_{amb}) is the absorbed atmospheric radiant energy, $P_{cond+conv}$ is the convection and conduction power density on the surface of the radiative cooling material, where the combined non-radiative heat coefficient ($\mathrm{h_c}$) is limited to 0, 4, 10 W/m^2/K. These parameters can be calculated by the following equation:

$$\mathrm{P}_{\mathrm{r}\,ad}(T) = A2\pi\int_0^{\frac{\pi}{2}} d\Omega \sin\theta\cos\theta\int_{2.5}^{25} d\lambda I_B(\lambda,T)\varepsilon(\lambda,\theta) \quad \backslash*$$

MERGEFORMAT (2)

$$I_B(\lambda,T) = \frac{2hc^2}{\lambda^5\left(e^{\frac{hc}{\lambda K_B T}} - 1\right)} \quad \backslash*$$

MERGEFORMAT (3)

Where $2\pi\int_0^{\frac{\pi}{2}} d\Omega \sin\theta$ is the angular integral over a hemisphere. ε (λ, θ) is the directional emissivity of the surface at wavelength λ. I_B (λ, T) is the spectral radiance of a blackbody at temperature T. h is Planck's constant, K_B is the Boltzmann constant, and C is the speed of light.

$$P_{atm}(T_{amb}) = A2\pi\int_0^{\frac{\pi}{2}} d\Omega \sin\theta\cos\theta\int_0^{\infty} d\lambda I_B(\lambda, T_{amb})\varepsilon_{amb}(\lambda,\theta) \quad \textbf{(4)}$$

$$\varepsilon_{amb}(\lambda,\theta) = 1-\tau(\lambda)^{\frac{1}{con\theta}} \quad \textbf{(5)}$$

Where $\varepsilon_{amb}(\lambda,\theta)$ is the angle-dependent emissivity of the atmosphere; τ(λ) is the atmospheric transmittance in the zenith direction.

$$P_{sun} = A\int_0^{\infty} d\lambda\varepsilon\left(\lambda,\theta_{sun}\right)I_{AM1.5}(\lambda) \quad \textbf{(6)}$$

Where θ_{sun} is the angle of incidence of sunlight incident on the radiation-cooling film, the solar illumination is represented by the AM1.5 spectrum ($I_{AM1.5}$(λ)).

$$P_{cond+conv}(T,T_{amb}) = Ah_c(T_{amb}-T) \quad \backslash*$$

MERGEFORMAT (7)

Reference

(1) P. Salehikahrizsangi, K. Raeissi, F. Karimzadeh, L. Calabrese and E. Proverbio, Applied Surface Science, 2020, **520**, 146319.

(2) M.Żenkiewicz, Journal of Achievements in Materials and Manufacturing Engineering, 2007, **24**, 137-145.

(3) H. Yang, J. Zhou, Z. Duan, B. Lu, B. Deng and W. Xu, *ACS Applied Materials & Interfaces*, 2022, **14**, 3244-3254.

(4) C. Chen, X. Jia, X. Li, M. Shi, J. Hu, M. Song, S. Wu, H. Dai, X. Wang and H.

Geng, *Chemical Engineering Journal*, 2023, **475**, 146307.

(5) X. Yu, W. Song, Q. Yu, S. Li, M. Zhu, Y. Zhang, W. Deng, W. Yang, Z. Huang and X. Bi, *Journal of environmental sciences*, 2018, **71**, 76-88.

(6) J. Liu, Y. Zhang, S. Li, C. Valenzuela, S. Shi, C. Jiang, S. Wu, L. Ye, L. Wang and Z. Zhou, *Chemical Engineering Journal*, 2023, **453**, 139739.